Hindawi
Journal of Engineering
Volume 2018, Article ID 4989584, 6 pages
https://doi.org/10.1155/2018/4989584

Research Article

Analysis of Isolation Ground Vibration by Graded Wave Impeding Block under a Moving Load

Qiang Ma and Feng-xi Zhou

School of Civil Engineering, Lanzhou University of Technology, Lanzhou, Gansu 730050, China

Correspondence should be addressed to Feng-xi Zhou; 1303110614@qq.com

Received 11 May 2018; Accepted 9 July 2018; Published 1 August 2018

Academic Editor: Lucian Dascalescu

Combined with the coordinate transformation, the dynamic governing equations for elastic foundation under a moving load are established by using the reverberation ray matrix method, and the isolation effect of a graded wave impeding block is studied. The displacement and the stress are obtained in the time domain by using numerical inverse Fourier transformation. Via numerical examples, the effectiveness of vibration isolation of graded wave impeding block is compared to conventional single phase solid homogenous wave impeding block. The results show that compared with the single phase solid homogenous wave impeding block isolation system, the graded wave impeding block can effectively reduce the vibration amplitude and has more advantages and is effective under a moving load.

1. Introduction

With the rapid development of urbanization and modern industry, ground vibration caused by moving load is becoming more and more frequent and it has become public considerable attention and engineering concern [1]. Therefore, numerous studies have been conducted on the vibration isolation induced by moving loads. For a moving load, there are different ways to reduce the ground vibrations [2]. For example, the effectiveness of three different wave barriers, namely, the open trench, in-filled trench, and elastic foundation, in reducing the ground vibrations caused by the passage of trains is studied [3–7], which indicate that open trenches are more efficient than in-filled trenches or soil stiffening-even at low frequencies.

Besides barrier for isolating vibration, artificial setting of the wave impedance block (WIB) in the foundation to study the vibration isolation performance of vibration control has made great progress. Chouw and Schmid [8, 9] firstly suggested placing an artificial bed rock called "wave impeding block" (WIB) under the vibration foundation to screen the low frequency vibrations in the wave propagation regime. Their results showed that the WIB was more effective at low frequencies than a buried wall barrier of similar dimensions. Peplow [10] investigated the vibration isolation of WIB in the far-field of the surface of the ground due to a harmonic load acting over a strip by boundary element (BE) method. Takemiya [11] studied the response on the surface of the ground in the time domain with a Ricker wavelet type loading by using a boundary element model; their results showed that an effective width of the WIB should be chosen in relation to the wavelength of the given load. Based on a semianalytical BEM, the vibration effect of WIB in stratified half-space under the load of the travelling train is analyzed by Gao [12, 13].

It should be noted that WIB vibration isolation system as an effective measure for vibration pollution control is applied in practical engineering, but the previous studies mostly focused on the homogenous materials; few research works have been conducted on the vibration isolation performance of wave impeding block with materials properties that have a continuous variation along space relatively [14]. As we all know, the functionally graded materials (FGMs) have the advantages of relieving thermal stress, avoiding or reducing

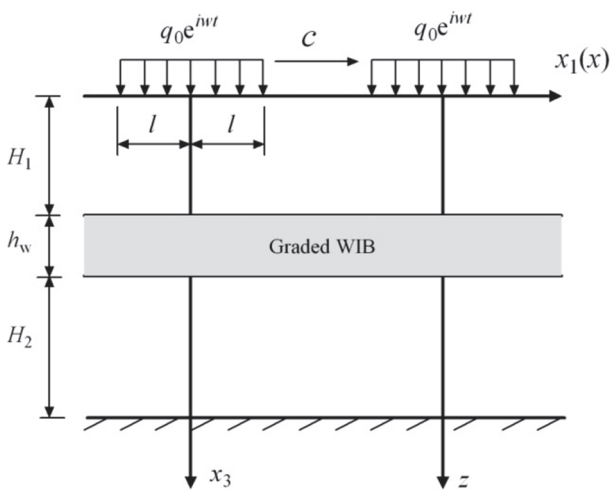

Figure 1: Physical model of elastic soil foundation under moving load.

stress concentration, and being well designed [15, 16]. In particular, the gradient factor of FGMs has a significant influence on the dispersion curve and attenuation curve of the wave and causes the dissipation of energy in the process of vibration [17].

In this study, based on the FGMs, the isolation effect of graded WIB on reducing vibration induced by a moving load in elastic foundations is studied. This paper is organized as follows: combined with the coordinate transformation, the dynamic governing equations for elastic foundation under a moving load are established in Section 2. Using the reverberation ray matrix method (RRMM), the expressions of displacement and stress in the frequency domain are derived to study the vibration isolation of graded WIB in Section 3. Section 4 shows the effectiveness of vibration isolation of graded WIB compared to the homogenous WIB and without WIB via the numerical example. Finally, the conclusion is drawn in Section 5.

2. General Solution of Elastic Medium under Moving Load

Considering setting the graded WIB in elastic foundations subjected to a moving load as depicted in Figure 1, the thickness of foundations is $H = H_1 + h_w + H_2$, where the thickness of graded WIB is h_w, the upper layer has a thickness H_1, and the lower layer has a thickness H_2 in x_3 direction. A moving load, which moves in the x_1-direction at constant speed c, rests on a homogenous elastic soils stratum; the load amplitude is q_0, the distribution length is $2l.(x_1, x_3)$ is Cartesian coordinate, and (x, z) is the moving coordinate which moves in the x_1-direction with moving load at constant speed c.

The basic equations for elastic medium are as follows: equations of motion:

$$\sigma_{ij} = \lambda e \delta_{ij} + 2\mu \varepsilon_{ij} \tag{1}$$

strain-displacement relationship:

$$\varepsilon_{ij} = \frac{1}{2}\left(u_{i,j} + u_{j,i}\right) \tag{2}$$

constitutive law:

$$\sigma_{ij,j} = \rho \ddot{u}_i. \tag{3}$$

In the above equations, σ_{ij} $(i, j = 1, 3)$ are stress components, respectively. δ_{ij} is the Dirac delta function, u_i represents the components of displacements, $e = u_{i,i}$, ε_{ij} denotes the strain components, ρ is the density, and λ and μ are Lamé constants.

In the absence of body forces, these can be written as

$$\mu \nabla^2 u + (\mu + \lambda) \nabla e = \rho \ddot{u}. \tag{4}$$

In order to solve governing equation (4), according to the Helmholtz decomposition method, the displacements vectors $\mathbf{u}(x_1, x_3)$ are represented by scalar and vector potentials as follows:

$$\mathbf{u} = \nabla \varphi + \nabla \times \psi. \tag{5}$$

Substituting the above resolutions into (4), we obtain two sets of coupled equation in terms of the scalar potentials as follows:

$$(2\mu + \lambda) \nabla^2 \varphi = \rho \frac{\partial^2 \varphi}{\partial t^2} \tag{6a}$$

$$\mu \nabla^2 \psi = \rho \frac{\partial^2 \psi}{\partial t^2}. \tag{6b}$$

The displacement vectors in the Cartesian coordinate (x_1, x_3) and the scalar potentials ϕ and ψ can be expressed as the harmonic functions of the angular frequency in the case of steady state by introducing the moving coordinate (x, z); i.e., $x_1 = x - ct$, $x_3 = z$.

$$u_1(x_1, x_3, t) = u_x(x - ct, z, t)\, e^{i\omega t} \tag{7a}$$

$$u_3(x_1, x_3, t) = u_z(x - ct, z, t)\, e^{i\omega t} \tag{7b}$$

$$\chi(x_1, x_3, t) = \chi(x - ct, z, t)\, e^{i\omega t} \tag{7c}$$

where $\chi = [\varphi, \psi]$.

Thus, the derivatives are changed as follows:

$$\dot{\chi}(x - ct, z, t) = (i\omega\chi - c\chi_{,x})\, e^{i\omega t} \tag{8a}$$

$$\ddot{\chi}(x - ct, z, t) = \left(-\omega^2\chi - 2i\omega c\chi_{,x} + c^2\chi_{,xx}\right) e^{i\omega t} \tag{8b}$$

where the subscript $\chi_{,x}$, $\chi_{,xx}$ denotes the partial differentiation with respect to x.

The Fourier transform with respect to x is defined as

$$\tilde{f}(\xi, z) = \int_{-\infty}^{\infty} f(x, z)\, e^{-i\xi x} dx. \tag{9}$$

Performing the Fourier transform with respect to the horizontal coordinates x on (6a) and (6b), the governing (6a) and (6b) can be uncoupled as

$$\frac{\partial^2 \tilde{\varphi}}{\partial z^2} - \alpha^2 \tilde{\varphi} = 0 \tag{10}$$

$$\frac{\partial^2 \tilde{\psi}}{\partial z^2} - \beta^2 \tilde{\psi} = 0 \tag{11}$$

where $\alpha = \sqrt{\xi^2 - \alpha_1/c_p^2}$, $\beta = \sqrt{\xi^2 - \alpha_1/c_s^2}$, $\alpha_1 = \omega^2 - 2c\omega\xi + c^2\xi^2$, $c_p = \sqrt{(\lambda + 2\mu)/\rho}$, $c_s = \sqrt{\mu/\rho}$.

Therefore, solution of the ordinary differential equations in (10) and (11) yields the following general solutions for the Fourier transform domain potentials:

$$\tilde{\varphi} = A_1(\xi, \omega)\, e^{\alpha z} + B_1(\xi, \omega)\, e^{-\alpha z} \tag{12}$$

$$\tilde{\psi} = A_2(\xi, \omega)\, e^{\beta z} + B_2(\xi, \omega)\, e^{-\beta z}. \tag{13}$$

In the moving coordinate (x, z), the displacement can be expressed by using the potentials φ and ψ:

$$u_x = \frac{\partial \varphi}{\partial x} - \frac{\partial \psi}{\partial z} \tag{14a}$$

$$u_z = \frac{\partial \varphi}{\partial z} + \frac{\partial \psi}{\partial x} \tag{14b}$$

Combining (12), (13), (14a), (14b), and (1), the generation solution of the displacement and stress of the dynamic of soil in the Fourier transform domain can be obtained:

$$\tilde{u}_x = i\xi\left(A_1 e^{\alpha z} + B_1 e^{-\alpha z}\right) - \beta\left(A_2 e^{\beta z} - B_2 e^{-\beta z}\right) \tag{15a}$$

$$\tilde{u}_z = \alpha\left(A_1 e^{\alpha z} - B_1 e^{-\alpha z}\right) + i\xi\left(A_2 e^{\beta z} + B_2 e^{-\beta z}\right) \tag{15b}$$

$$\tilde{\sigma}_z = g\left(A_1 e^{\alpha z} + B_1 e^{-\alpha z}\right) + 2i\mu\xi\beta\left(A_2 e^{\beta z} - B_2 e^{-\beta z}\right) \tag{15c}$$

$$\begin{aligned}\tilde{\sigma}_{xz} = \mu\Big[&2i\xi\alpha\left(A_1 e^{\alpha z} - B_1 e^{-\alpha z}\right) \\ &- \left(\beta^2 + \xi^2\right)\left(A_2 e^{\beta z} + B_2 e^{-\beta z}\right)\Big]\end{aligned} \tag{15d}$$

where $g = 2\mu\alpha^2 + \lambda(\alpha^2 - \xi^2)$.

3. Reverberation Ray Matrix Method

It is usually very difficult to obtain analytical solutions to the governing equations for waves in a general graded WIB. When the material properties vary with the thickness coordinate only, we can adopt an accurate laminate plate to model the original graded WIB as shown in Figure 2 [18]; the graded WIB is divided into many layers of small thickness so that the material properties of each layer can be regarded as constant. The number of layers, N, is controlled by the accuracy of the model [18]. In recent years, RRMM is a new solution method which was originally developed by Pao et al. [19], who further [20] applied it to study the transient wave propagation in layered liquids as well as in laminated solids, and it has been demonstrated that RRMM has a great advantage in tracing the wave rays. In this paper, RRMM will be employed to analyze the graded WIB. One key step in RRMM is that two local coordinates should be employed for each layer. One locates at the upper surface of the layer and the other locates at the lower surface. Figure 3 shows the two local coordinates at the ith interface. The superscript of the coordinate $(x^{i(i-1)}, z^{i(i-1)})$ indicates that it locates at the ith interface and directs to the (i-1)th interface.

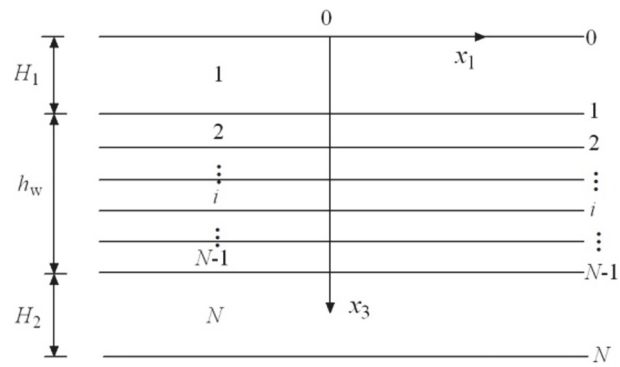

Figure 2: The approximate laminate model of graded WIB.

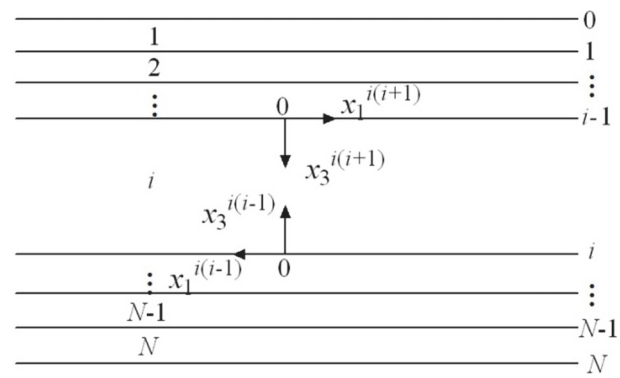

Figure 3: Dual local coordinates at the interface.

In the local coordinates $(x^{i(i-1)}, 0)$, according to (15a), (15b), (15c), and (15d), we have the solution as follows:

$$\tilde{u}_x^{i(i-1)} = i\xi\left(A_1^{i(i-1)} + B_1^{i(i-1)}\right) - \beta_i\left(A_2^{i(i-1)} - B_2^{i(i-1)}\right) \tag{16a}$$

$$\tilde{u}_z^{i(i-1)} = \alpha_i\left(A_1^{i(i-1)} - B_1^{i(i-1)}\right) + i\xi\left(A_2^{i(i-1)} + B_2^{i(i-1)}\right) \tag{16b}$$

$$\tilde{\sigma}_z^{i(i-1)} = g_i\left(A_1^{i(i-1)} + B_1^{i(i-1)}\right) + 2i\mu\xi\beta_i\left(A_2^{i(i-1)} - B_2^{i(i-1)}\right) \tag{16c}$$

$$\tilde{\sigma}_{xz}^{i(i-1)} = \mu\left[2i\xi\alpha_i\left(A_1^{i(i-1)} - B_1^{i(i-1)}\right) - \left(\beta_i^2 + \xi^2\right)\left(A_2^{i(i-1)} + B_2^{i(i-1)}\right)\right]. \tag{16d}$$

At the ith interface, the continuity conditions require

$$\tilde{u}_x^{i(i-1)} = -\tilde{u}_x^{i(i+1)}, \quad \tilde{u}_z^{i(i-1)} = -\tilde{u}_z^{i(i+1)} \tag{17a}$$

$$\tilde{\sigma}_z^{i(i-1)} = \tilde{\sigma}_z^{i(i+1)}, \quad \tilde{\sigma}_{xz}^{i(i-1)} = \tilde{\sigma}_{xz}^{i(i+1)}. \tag{17b}$$

By virtue of (16a), (16b), (16c), (16d), (17a), and (17b), we get the so-called local scattering relations at the ith interface written in a matrix form as

$$\mathbf{A}^i = \mathbf{S}^i\mathbf{B}^i \quad (i = 1, 2, \cdots N-1) \tag{18}$$

where $\mathbf{A}^i = \left[A_1^{i(i-1)}\ A_2^{i(i-1)}\ A_1^{i(i+1)}\ A_2^{i(i+1)}\right]^{\mathrm{T}}$ is the amplitude vector of departing waves; $\mathbf{B}^i = \left[B_1^{i(i-1)}\ B_2^{i(i-1)}\ B_1^{i(i+1)}\ B_2^{i(i+1)}\right]^{\mathrm{T}}$ is the amplitude vector of arriving waves; the matrix $\mathbf{S}^i$ is called the scattering matrix at ith interface; and

$$\mathbf{S}^i = \begin{bmatrix} i\xi & -\beta_i & i\xi & -\beta_{i+1} \\ \alpha_i & i\xi & \alpha_{i+1} & i\xi \\ g_i & 2i\mu\xi\beta_i & -g_{i+1} & -2i\mu\xi\beta_{i+1} \\ 2i\xi\alpha_i & -\left(\beta_i^2+\xi^2\right) & -2i\xi\alpha_{i+1} & \left(\beta_{i+1}^2+\xi^2\right) \end{bmatrix}^{-1} \cdot \begin{bmatrix} -i\xi & -\beta_i & -i\xi & -\beta_{i+1} \\ \alpha_i & -i\xi & \alpha_{i+1} & -i\xi \\ -g_i & 2i\mu\xi\beta_i & g_{i+1} & -2i\mu\xi\beta_{i+1} \\ 2i\xi\alpha_i & \left(\beta_i^2+\xi^2\right) & -2i\xi\alpha_{i+1} & -\left(\beta_{i+1}^2+\xi^2\right) \end{bmatrix}. \tag{19}$$

Considering that the soil foundation surface subjected to a moving load and the bottom surface is fixed, the appropriate boundary conditions to be satisfied in the frequency domain and moving coordinate frame are given by

$$\text{at } z = 0: \quad \tilde{\sigma}_z = -q_0\frac{\sin(\xi l)}{\xi l}, \ \tilde{\sigma}_{xz} = 0 \tag{20a}$$

$$\text{at } z = H: \quad \tilde{u}_x = 0, \ \tilde{u}_z = 0. \tag{20b}$$

By substituting (20a) and (20b) into (16a), (16b), (16c), and (16d), we can obtain

$$\mathbf{A}^0 = \mathbf{S}^0\mathbf{B}^0 + \mathbf{Q}^0 \tag{21a}$$

$$\mathbf{A}^N = \mathbf{S}^N\mathbf{B}^N \tag{21b}$$

where $\mathbf{A}^0 = \left[A_1^{01}\ A_2^{01}\right]^{\mathrm{T}}$, $\mathbf{B}^0 = \left[B_1^{01}\ B_2^{01}\right]^{\mathrm{T}}$, $\mathbf{Q}^0 = \left[\tilde{q}(\xi)\ 0\right]^{\mathrm{T}}$, $\mathbf{A}^N = \left[A_1^{N(N-1)}\ A_2^{N(N-1)}\right]^{\mathrm{T}}$, $\mathbf{B}^N = \left[B_1^{N(N-1)}\ B_2^{N(N-1)}\right]^{\mathrm{T}}$, $\mathbf{S}^N = \begin{bmatrix} i\xi & -\beta_N \\ \alpha_N & i\xi \end{bmatrix}^{-1}\begin{bmatrix} -i\xi & -\beta_N \\ \alpha_N & -i\xi \end{bmatrix}$ $\mathbf{S}^0 = \begin{bmatrix} g_1 & 2i\mu\xi\beta_1 \\ 2i\xi\alpha_1 & -(\beta_1^2+\xi^2) \end{bmatrix}^{-1}\begin{bmatrix} -g_1 & 2i\mu\xi\beta_1 \\ 2i\xi\alpha & (\beta_1^2+\xi^2) \end{bmatrix}$.

Combination of (18) , (21a), and (21b) leads to

$$\mathbf{A} = \mathbf{S}\mathbf{B} + \mathbf{Q} \tag{22}$$

where $\mathbf{A} = \left[(\mathbf{A}^0)^{\mathrm{T}}\ (\mathbf{A}^1)^{\mathrm{T}}\ \cdots\ (\mathbf{A}^{N-1})^{\mathrm{T}}\ (\mathbf{A}^N)^{\mathrm{T}}\right]^{\mathrm{T}}$, $\mathbf{B} = \left[(\mathbf{B}^0)^{\mathrm{T}}\ (\mathbf{B}^1)^{\mathrm{T}}\ \cdots\ (\mathbf{B}^{N-1})^{\mathrm{T}}\ (\mathbf{B}^N)^{\mathrm{T}}\right]^{\mathrm{T}}$, $\mathbf{S} = \begin{bmatrix} \mathbf{S}_{2\times2}^0 & 0_{2\times4} & 0_{2\times4} & \cdots & 0_{2\times4} & 0_{2\times2} \\ 0_{4\times2} & \mathbf{S}_{4\times4}^1 & 0_{4\times4} & \cdots & 0_{4\times4} & 0_{4\times2} \\ 0_{4\times2} & 0_{4\times4} & \mathbf{S}_{4\times4}^2 & \cdots & 0_{4\times4} & 0_{4\times2} \\ \vdots & \vdots & \vdots & \ddots & \vdots & \vdots \\ 0_{4\times2} & 0_{4\times4} & 0_{4\times4} & \cdots & \mathbf{S}_{4\times4}^{N-1} & 0_{4\times2} \\ 0_{2\times2} & 0_{2\times4} & 0_{2\times4} & \cdots & 0_{2\times4} & \mathbf{S}_{2\times2}^N \end{bmatrix}$.

Equation (22) presents a global scattering relation between various waves at all interfaces and two boundary surfaces. It is shown that (22) contains a total of $4N$ algebraic equations with totally $8N$ unknowns. Thus, additional relations should be supplemented. Notice that a departing wave in the local coordinates $(x^{i(i-1)}, z^{i(i-1)})$ becomes an arriving wave in the local coordinates $(x^{i(i-1)}, z^{i(i-1)})$. Hence, we can deduce the following phase relations:

$$\tilde{u}_z^{i(i-1)}(z) = -\tilde{u}_z^{(i-1)i}\left(\tilde{h}_i - z\right) \tag{23}$$

where $\tilde{h}_i$ is ith thickness.

By substituting (16b) into (23), we can obtain

$$\begin{bmatrix} B_1^{(i-1)i} \\ B_2^{(i-1)i} \\ B_1^{i(i-1)} \\ B_2^{i(i-1)} \end{bmatrix} = \begin{bmatrix} e^{\alpha_i\tilde{h}_i} & 0 & 0 & 0 \\ 0 & -e^{\beta_i\tilde{h}_i} & 0 & 0 \\ 0 & 0 & e^{\alpha_i\tilde{h}_i} & 0 \\ 0 & 0 & 0 & -e^{\beta_i\tilde{h}_i} \end{bmatrix}\begin{bmatrix} A_1^{i(i-1)} \\ A_2^{i(i-1)} \\ A_1^{(i-1)i} \\ A_2^{(i-1)i} \end{bmatrix}. \tag{24}$$

Introducing a new departing wave vector,

$$\tilde{\mathbf{A}} = \left[A_1^{10}\ A_2^{10}\ A_1^{01}\ A_2^{01}\ \cdots\ A_1^{N(N-1)}\ A_2^{N(N-1)}\ A_1^{(N-1)N}\ A_2^{(N-1)N}\right]. \tag{25}$$

Combining (22), (24), and (25), we can obtain

$$\mathbf{B} = \mathbf{P}\widetilde{\mathbf{A}}, \qquad \widetilde{\mathbf{A}} = \mathbf{U}\mathbf{A} \tag{26}$$

where $\mathbf{P}$ is the phase matrix defined by

$$\mathbf{P} = \begin{bmatrix} \mathbf{P}^{01} & 0_{4\times4} & \cdots & 0_{4\times4} \\ 0_{4\times4} & \mathbf{P}^{12} & \cdots & 0_{4\times4} \\ \vdots & \vdots & \ddots & \vdots \\ 0_{4\times4} & 0_{4\times4} & \cdots & \mathbf{P}^{N(N-1)} \end{bmatrix},$$
$$\mathbf{P}^{(i-1)i} = \begin{bmatrix} e^{\alpha_i \tilde{h}_i} & 0 & 0 & 0 \\ 0 & -e^{\beta_i \tilde{h}_i} & 0 & 0 \\ 0 & 0 & e^{\alpha_i \tilde{h}_i} & 0 \\ 0 & 0 & 0 & -e^{\beta_i \tilde{h}_i} \end{bmatrix}. \tag{27}$$

It can be seen that the elements in $\widetilde{\mathbf{A}}$ are completely the same as those in $\mathbf{A}$, but the orders of elements change. Therefore, we can introduce the permutation matrix $\mathbf{U}$ to link them together and define them by

$$\mathbf{U} = \begin{bmatrix} \mathbf{U}^0 & 0_{4\times4} & \cdots & 0_{4\times4} \\ 0_{4\times4} & \mathbf{U}^0 & \cdots & 0_{4\times4} \\ \vdots & \vdots & \ddots & \vdots \\ 0_{4\times4} & 0_{4\times4} & \cdots & \mathbf{U}^0 \end{bmatrix},$$
$$\mathbf{U}^0 = \begin{bmatrix} 0 & 0 & 1 & 0 \\ 0 & 0 & 0 & 1 \\ 1 & 0 & 0 & 0 \\ 0 & 1 & 0 & 0 \end{bmatrix}. \tag{28}$$

It is then obtained by substituting (27) into (23) that

$$\mathbf{A} = [\mathbf{I} - \mathbf{R}]^{-1}\mathbf{Q}, \qquad \mathbf{B} = \mathbf{PUA} \tag{29}$$

where $\mathbf{R}$ **is** the reverberation matrix defined by $\mathbf{R} = \mathbf{SPU}$ and $\mathbf{I}$ is the unit matrix.

Finally, solving (29), we can obtain $\mathbf{A}$ and $\mathbf{B}$. Combining (16a), (16b), (16c), and (16d), the displacement and stress of the dynamic of soil in the frequency domain can be obtained, and then the corresponding physical quantities in the Fourier transform domain are obtained by applying the inverse Fourier transform.

4. The Numerical Example and Discussion

Assuming that the material properties of graded wave impeding block have an exponential law distribution along the thickness coordinate, there are

$$G(z) = [G(0) - G(z)]\left(\frac{H-z}{H}\right)^{\gamma} + G(H) \tag{30}$$

Table 1: Physical-mechanical parameters of surface and bottom of graded WIB.

Location	E/Pa	ρ/ (g/cm^3)	ν
Surface	6.5×10^6	1.4	0.3
Bottom	6.5×10^8	2.458	0.33

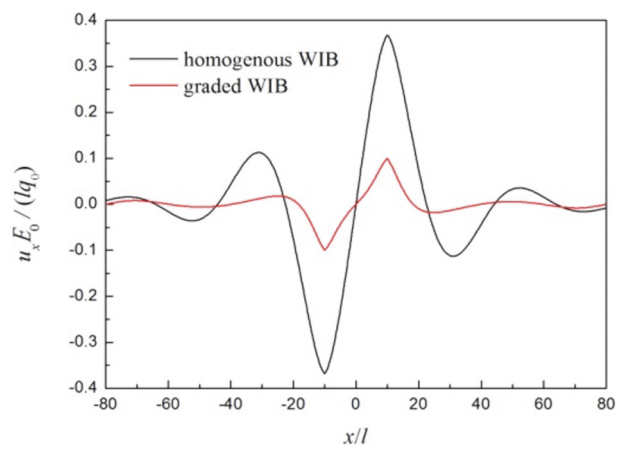

Figure 4: Variations of u_x at the ground surface.

where $G(x_3)$ represents the physical-mechanical parameters of graded WIB; γ is a nonhomogeneous parameter, named gradient index, and different values of γ dictate that the material properties have different nonhomogeneous distributions through the thickness of WIB. From (30) we can know that graded materials become homogenous materials when $\gamma = 0$.

The physical and mechanical parameters of elastic soil foundation are as follows [21]: $E_0 = 7.7 \times 10^7$Pa, $\nu = 0.35$, $\rho_0 = 1.816$g/cm^3. The parameters $l = 0.5$m, $H_1 = 3$m, $h_w = 3$m, $c = 100$m/s, $\omega = 16$rad/s, $q_0 = 1$kPa are used in the following analysis. The physical-mechanical parameters of surface and bottom of graded WIB are shown in Table 1. For simplicity, assume that all physical-mechanical parameters of graded WIB have the same gradient index.

Figures 4-5 show the variations of horizontal displacement u_x and vertical displacement u_z along the horizontal direction at the ground surface with the homogenous WIB (where the gradient index $\gamma = 0$) and the graded WIB (where the gradient index $\gamma = 5$). Comparing between the homogenous WIB and graded WIB, from Figures 4 and 5, we can see that the graded WIB has changed the vibration phase of horizontal displacement u_x and vertical displacement u_z. Meanwhile, it is shown in Figures 4 and 5 that the u_x and $u_z$values at the ground surface in a graded WIB are much less than those in a homogeneous WIB. The maximum u_x value is 0.368 when $\gamma = 0$, while the maximum u_x value is 0.099 when $\gamma = 5$; the maximum u_z value is 4.032 when $\gamma = 0$, while the maximum u_z value is 1.168 when $\gamma = 5$. It indicates that the amplitude of u_x and u_z is significantly reduced with the graded WIB, indicating a better vibration isolation of the graded WIB.

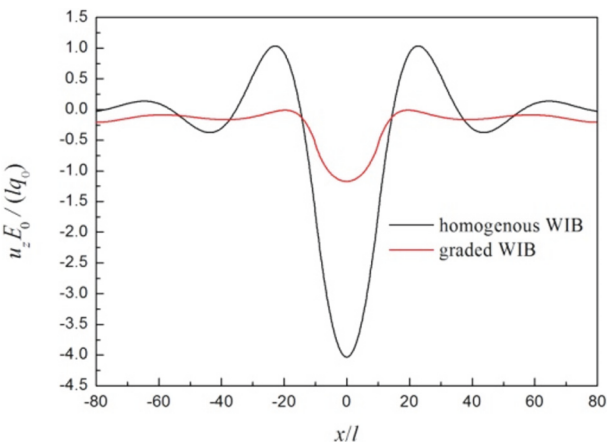

Figure 5: Variations of u_z at the ground surface.

5. Conclusions

In this study, based on the FGMs, the isolation effect of graded WIB on reducing vibration induced by a moving load in elastic foundations is studied. Combined with the coordinate transformation, using the reverberation ray matrix method, the expressions of displacement and stress in the frequency domain are derived to study the vibration isolation of graded WIB. Based on the numerical example in this paper, the result shows that the u_x and $u_z$values when $\gamma = 5$ are smaller than those when $\gamma = 0$; it is interesting to note that the vibration isolation of the graded WIB is better than that of the homogeneous WIB.

Data Availability

The data used to support the findings of this study are available from the corresponding author upon request.

Conflicts of Interest

The authors declare that they have no conflicts of interest.

Acknowledgments

This work was supported by the Chinese Natural Science Foundation (Grant no. 51368038).

References

[1] h. Xia and Y.-m. Cao, "Problem of railway traffic induced vibrations of environments," *Journal of Railway Science and Engineering*, vol. 1, no. 1, pp. 44–51, 2004.

[2] E. Çelebi, S. Firat, G. Beyhan, I. Çankaya, I. Vural, and O. Kirtel, "Field experiments on wave propagation and vibration isolation by using wave barriers," *Soil Dynamics and Earthquake Engineering*, vol. 29, no. 5, pp. 824–833, 2009.

[3] Y.-B. Yang and H.-H. Hung, "A parametric study of wave barriers for reduction of train-induced vibrations," *International Journal for Numerical Methods in Engineering*, vol. 40, no. 20, pp. 3729–3747, 1997.

[4] L. Andersen and S. R. K. Nielsen, "Reduction of ground vibration by means of barriers or soil improvement along a railway track," *Soil Dynamics and Earthquake Engineering*, vol. 25, no. 7–10, pp. 701–716, 2005.

[5] C. With, M. Bahrekazemi, and A. Bodare, "Wave barrier of lime-cement columns against train-induced ground-borne vibrations," *Soil Dynamics and Earthquake Engineering*, vol. 29, no. 6, pp. 1027–1033, 2009.

[6] W. Yuan, Y.-Q. Cai, L. Shi, and Z.-G. Cao, "Study of vibration-isolation efficiency of open trench in saturated ground by 2.5D finite element method," *Yantu Lixue/Rock and Soil Mechanics*, vol. 34, no. 7, pp. 2111–2118, 2013.

[7] B. Zhen-ning, W. Jing-ya, and J.-w. Liang, "Reduction of train-induced vibrations by using a trench in a layered foundation," *Rock and Mechanics*, vol. 29, no. 5, pp. 861–873, 2016.

[8] N. Chouw, R. Le, and G. Schmid, "Propagation of vibration in a soil layer over bedrock," *Engineering Analysis with Boundary Elements*, vol. 8, no. 3, pp. 125–131, 1991.

[9] N. Chouw, R. Le, and G. Schmid, "An approach to reduce foundation vibrations and soil waves using dynamic transmitting behavior of a soil layer," *Bauingenieur*, vol. 66, pp. 215–221, 1991.

[10] A. T. Peplow, C. J. C. Jones, and M. Petyt, "Surface vibration propagation over a layered elastic half-space with an inclusion," *Applied Acoustics*, vol. 56, no. 4, pp. 283–296, 1999.

[11] H. Takemiya, "Field vibration mitigation by honeycomb WIB for pile foundations of a high-speed train viaduct," *Soil Dynamics and Earthquake Engineering*, vol. 24, no. 1, pp. 69–87, 2004.

[12] G.-Y. Gao, G.-Q. Chen, and B. Zhang, "Active vibration isolation using WIB in non-uniform ground under train loadings," *Zhendong yu Chongji*, vol. 32, no. 22, pp. 57–62, 2013.

[13] G.-Y. Gao, F. Wang, G.-Q. Chen, and B. Zhang, "Active vibration isolation of the saturated ground with wave impendence block inside and under the load of the travelling train," *Zhendong Gongcheng Xuebao*, vol. 27, no. 3, pp. 433–440, 2014.

[14] Ma. Qiang, F. Zhou, and J. Liu, "Analysis of ground vibration control by graded wave impeding block," *Chinese Journal of Theoretical and Applied Mechanics*, vol. 49, no. 6, pp. 1360–1369, 2017.

[15] W. Pompe, H. Worch, M. Epple et al., "Functionally graded materials for biomedical applications," *Materials Science and Engineering: A Structural Materials: Properties, Microstructure and Processing*, vol. 362, no. 1-2, pp. 40–60, 2003.

[16] Z. Zhong, L. Z. Wu, and W. Q. Chen, "Progress in the study on mechanics problems of functionally graded materials and structures," *Advances in Applied Mechanics*, vol. 40, no. 5, pp. 528–541, 2010.

[17] X. Kun, C. Mei-xia, and X. Kun, "Vibration analysis of orthotropic functionally graded plates," *Noise and Vibration Control*, vol. 36, no. 4, pp. 14–20, 2016.

[18] W. Q. Chen, H. M. Wang, and R. H. Bao, "On calculating dispersion curves of waves in a functionally graded elastic plate," *Composite Structures*, vol. 81, no. 2, pp. 233–242, 2007.

[19] Y. Pao, D. Keh, and S. M. Howard, "Dynamic response and wave propagation in plane trusses and frames," *AIAA Journal*, vol. 37, no. 5, pp. 594–603, 1999.

[20] X.-Y. Su, J.-Y. Tian, and Y.-H. Pao, "Application of the reverberation-ray matrix to the propagation of elastic waves in a layered solid," *International Journal of Solids and Structures*, vol. 39, no. 21-22, pp. 5447–5463, 2002.

[21] D. V. Jones, O. Laghrouche, D. Le Houedec, and M. Petyt, "Ground vibration in the vicinity of a rectangular load acting on a viscoelastic layer over a rigid foundation," *Journal of Sound and Vibration*, vol. 203, no. 2, pp. 307–319, 1997.